Microhydrodynamics Simulation of Single-collector Granular Filtration

Albert S. Kim*[1,2] and Seok-Tae Kang[3]

[1]Civil and Environmental Engineering, University of Hawaii at Manoa, Honolulu, Hawaii 96822, USA
[2]Chemical Engineering, Kyung Hee University, Gyeonggi-do 449-701, Korea
[3]Civil Engineering, Kyung Hee University, Gyeonggi-do 449-701, Korea

(Received May 14, 2012; CL-120594; E-mail: albertsk@hawaii.edu)

Granular filtration phenomenon is fundamentally investigated using dissipative hydrodynamics with a large collector grain and a non-Brownian sphere. Effects of interparticle forces balanced with hydrodynamic interactions are studied for particle trajectory analysis. In addition to conventional deposition of fine particles on collector surfaces (mostly near front hemispheres), the hydrodynamic trapping of rotating fine particles on the back hemisphere surface is fundamentally investigated using the exact solution of two-body hydrodynamics.

During the granular filtration process, fine particles transport to the vicinity of a spherical collector and attach to the collector surface under various physical and chemical conditions. For particles with a size less than 1 μm, Brownian diffusion is the primary transport mechanism owing to the tremendous number of bombardments from water molecules, which cause random drifting of particles. On the other hand, larger particles follow the flow streamlines and collide with collector surfaces (if the distance between streamline and collector surface is smaller than particle radius) and are captured due to an "interception" mechanism. In addition, if the particle mass is (significantly) heavier than that of water of the same volume, the gravitational force (minus the buoyant force) causes downward deviating motion from the streamline and leads the particles toward the upper hemispheres of capturing collectors; this mechanism is called "sedimentation" or "differential settling."

Yao et al.[1] (YHO) developed a conceptual model of granular filtration and indicated that particle transport during filtration is analogous to transport in the flocculation process (diffusion, interception, and sedimentation). A single-collector efficiency[2] is defined as $\eta = $ (particle strike ratio)$/v_0 C_0 \pi R_c^2$, where v_0 is the approaching fluid velocity, C_0 is the inlet concentration of particles to the filter, and R_c is the radius of the single collector. The efficiency is assumed to be a superposition of efficiencies of the individual mechanisms: $\eta = \eta_B + \eta_I + \eta_G$, where subscripts indicate Brownian (B), interception (I), and gravitation (G). Using the efficiency, the filter equation, derived as $\ln \frac{C}{C_0} = -\frac{3}{2} \varepsilon \alpha \eta (\frac{L}{d_c})$, is used to estimate particle removal efficiency, where ε is the bed porosity, α is the attachment probability, L is the filter length, d_c ($= 2R_c$) is the collector diameter, and C is the effluent concentration. The YHO theory used the Stokes–Einstein diffusivity and Stokes solution for fluid flow around a single sphere. Cookson's[3] approach was used to improve the prediction accuracy by applying Happel's correction factor A_s to η_D, i.e., $\eta_D \to A_s \eta_D$. The correction factor is represented as $A_s(\gamma) = 2(1 - \gamma^5)/W$ where $W = 2 - 3\gamma + 3\gamma^5 - \gamma^6$ and $\gamma^3 = 1 - \varepsilon$.

Rajagopalan and Tien[4] (RT) developed a fundamental theory and an empirical correlation using their simulation results. In addition to the three transport mechanisms proposed in the YHO model, RT included the London dispersion force and DLVO interactions.[5,6] The RT model aims to find a proper fluid mechanic model, which can include the effect of the porous media structure. Note that the YHO model considered a pair of particle and collector in an infinite fluid medium. Extending Cookson's[3] approach, RT incorporated Happel's sphere-in-cell model, where the tangential stress on the surface is assumed to be zero. Happel's correction factor A_s was mathematically retrieved in the RT theory. Instead of Stokes' flow profile, RT used stream functions that satisfy boundary conditions on the collector surface (no-slip) as well as the shell surface (no tangential stress). Stream function and fluid velocity were approximated with respect to the distance from the collector surface to the particle center. When Happel's correction factor was included, RT used $A_s^{1/3}$ following Cookson's[3] original approach, but YHO dropped the exponent $1/3$.

Tufenkji and Elimelech[7] (TE) readdressed the single-collector efficiency and proposed a theoretical representation with a new empirical correlation of higher accuracy. In the TE model, the diffusion efficiency (η_D) was calculated by solving the governing equation numerically after ignoring the primary particle size ($a_p \to 0$) and setting the particle density equal to the fluid density ($\rho_p = \rho_f$). This is because the contribution of diffusion to the rate of particle deposition cannot be disabled in the convection–diffusion equation. The interception and sedimentation efficiencies were calculated individually using a similar method by turning off other mechanisms in a sequence, and the total efficiency was represented as a linear sum of three individual efficiencies. In the numerical calculation of the TE model, the efficiency due to sedimentation barely changed with the bed porosity so that the porosity-dependent parameter A_s was dropped in the gravitational efficiency. In reality, these three mechanisms simultaneously influence multiparticle dynamics.

Nelson and Ginn[8] (NG) revisited the conventional colloidal filtration theory (CFT) and Happel's cell model using a direct numerical simulation of colloidal particles. In the Levich, YHO, and TE approaches, only a single collector was considered, as it is located in an infinite medium with a unidirectional flow field. The common practice between the YHO and TE models is that after the single-collector efficiency was calculated to numerically solving the convection–diffusion equation, Happel's correction factor A_s was selectively multiplied by individual efficiencies with physical intuition. Primarily, NG followed the trajectory analysis of RT's approach, but the fundamentality of using the trajectory analysis was significantly enhanced by including the Brownian force in the Langevin equation. The particle displacement from the current time t to $t + \delta t$ was assumed to be a superposition of deterministic and stochastic contributions, which are by nature proportional to δt and $\sqrt{\delta t}$,

respectively. Hydrodynamic drag coefficients were assumed to be constant, which may provide deviation from the true hydrodynamic interactions, especially near collector surfaces.

Conventional filtration theories discussed above must provide macroscopic quantities that can be verified with experimental observations such as particle removal efficiency or effluent concentration. Although all the models use a single collector with or without Happel's tangential-stress-free cell, the traveling particles are usually treated as point masses during Lagrangian-type dynamic simulations in RT and NG models. Eulerian simulations cannot include the angular motion of particles because the transient distribution of particles, i.e., particle concentration, is calculated in the YHO and TE models. While passing through interstitial void spaces of a granular bed, particles collide with collector surfaces. Strong attraction between the particle and collector induces deposition and attachment of the traveling particles with a certain probability, often experimentally measured. Weakly deposited particles can be detached, and they return to the bulk phase. Therefore, the particle's fate can be described using passing, attachment, and detachment. On the other hand, if a particle travels on the surface of a collector with a streamline from the front to back hemisphere, the net force exerted on the particle can be canceled out and the particle can be hydrodynamically trapped on the back hemisphere. In this case, the particle will stay at a specific location, undergoing continuous angular motion. We simulated this phenomenon using the exact two-body hydrodynamics.

The coupled N-body Langevin equation describes the three-dimensional motion of particle i of mass m_i and the moment of inertia I_i given an ambient flow field, $\mathbf{U}_\infty(\mathbf{r}) = \mathbf{V}_\infty + \mathbf{r} \times \mathbf{\Omega}_\infty + \mathbf{v}{:}\mathbf{E}$

$$\begin{bmatrix} m_i\mathbf{a}_i \\ I_i\boldsymbol{\alpha}_i \end{bmatrix} = \begin{bmatrix} \mathbf{F}_i^{\mathrm{Ex}} \\ \mathbf{T}_i^{\mathrm{Ex}} \end{bmatrix} - \begin{bmatrix} \mathbf{A}_{ij} & \tilde{\mathbf{B}}_{ij} \\ \mathbf{B}_{ij} & \mathbf{D}_{ij} \end{bmatrix} \begin{bmatrix} \Delta\mathbf{v}_j \\ \Delta\boldsymbol{\omega}_j \end{bmatrix} \quad (1)$$

where $\mathbf{a}_i/\boldsymbol{\alpha}_i$ are the translational/angular accelerations, $\mathbf{F}_i^{\mathrm{Ex}}/\mathbf{T}_i^{\mathrm{Ex}}$ is an external force/torque vector on the moving particle including the hydrodynamic stress (see below), the matrix is the grand resistance, and $\Delta\mathbf{v}_j (= \mathbf{v}_j - \mathbf{V}_\infty)$ and $\Delta\boldsymbol{\omega}_j (= \boldsymbol{\omega}_j - \mathbf{\Omega}_\infty)$ are the translational and angular velocities of particle j with respect to the unidirectional flow $\mathbf{V}_\infty$ and ambient vortice $\mathbf{\Omega}_\infty$, respectively. Here, we denote particle i as the traveling particle and j as the stationary particle. In our simulations, gravity was neglected and Brownian motion was turned off. The two-body hydrodynamic interactions already include lubrication forces and compete with the van der Waals attraction between the particle and the collector.

Hydrodynamic force/torque balance influencing the coupled inertia of translation and rotation, which were not discussed in NG model,[8] are

$$\begin{bmatrix} \mathbf{F}_i \\ \mathbf{T}_i \\ \mathbf{S}_i \end{bmatrix} = \begin{bmatrix} \mathbf{A} & \tilde{\mathbf{B}} & \tilde{\mathbf{G}} \\ \mathbf{B} & \mathbf{C} & \tilde{\mathbf{H}} \\ \mathbf{G} & \mathbf{H} & \mathbf{M} \end{bmatrix}_{ij} \begin{bmatrix} \Delta\mathbf{v}_j \\ \Delta\boldsymbol{\omega}_j \\ -\boldsymbol{e}_\infty \end{bmatrix} \quad (2)$$

where $\mathbf{F}_i$, $\mathbf{T}_i$, and $\mathbf{S}_i$ are hydrodynamic force, torque, and stresslet, respectively. Let $\boldsymbol{e}_\infty = (E_{xx} - E_{yy}, 2E_{xy}, 2E_{xz}, 2E_{yz}, E_{yy} - E_{zz})$ be the rate of strain, where $E_{ij} = \frac{1}{2}(\partial v_i/\partial x_j + \partial v_j/\partial x_i)$, which is symmetric and traceless, i.e., $E_{ij} = E_{ji}$ and $\sum_i E_{ij} = 0$, respectively. Therefore, one rewrites eq 2 as

$$\begin{bmatrix} \mathbf{F}_i \\ \mathbf{T}_i \end{bmatrix} = - \begin{bmatrix} \mathbf{A} & \tilde{\mathbf{B}} \\ \mathbf{B} & \mathbf{C} \end{bmatrix}_{ij} \begin{bmatrix} \Delta\mathbf{v}_j \\ \Delta\boldsymbol{\omega}_j \end{bmatrix} - \begin{bmatrix} \tilde{\mathbf{G}} \\ \tilde{\mathbf{H}} \end{bmatrix}_{ij} [\boldsymbol{e}_\infty] \quad (3)$$

We took the second term of eq 3 as external force/torque, $[\mathbf{F}_i^{\mathrm{Ex}}, \mathbf{T}_i^{\mathrm{Ex}}]^T$, in eq 1. In spherical coordinates with the origin at the collector center, the rate of strain has the following components:

$$E_{rr} = +\frac{U_\circ \cos\theta}{R}\left[\left(\frac{R}{r}\right)^2 - \left(\frac{R}{r}\right)^4\right] = -2E_{\theta\theta} = -2E_{\phi\phi} \quad (4)$$

$$E_{r\theta} = E_{\theta r} = -\frac{3U_\circ}{2a}\sin\theta\left(\frac{R}{r}\right)^4 \quad (5)$$

and

$$E_{\theta\phi} = E_{r\phi} = 0 \quad (6)$$

Equations 4–6 are converted to Cartesian coordinates and used in eq 3 to calculate the external influences on particle dynamics due to the rate of strain. For numerical integration of the governing equation, the inertial and drag forces are scaled using $m_0 V_\infty/a_0$ and $6\pi\mu a_0 V_\infty$, and the drag-to-inertial ratio is set to 10^4, where m_0 and a_0 are the mass and radius of the smallest particle, respectively. This corresponds to a standard case of the primary particle radius of $a_{\mathrm{p}} = 4.5\,\mu\mathrm{m}$ and approaching speed of $U_0 = 10^{-4}\,\mathrm{m\,s^{-1}}$.

Figure 1 shows the trajectory of a fine particle around the collector. To exemplify this phenomenon, we set the collector size at 10 times the particle size. The collector is fixed at the origin of the reference frame, and the particle is initially located on top of the collector with the same horizontal velocity of the ambient flow. The particle maintains a certain distance from the collector surface as it moves down following the fluid flow. Interestingly, the particle does cross the horizontal line passing through the center of the spherical collector. The nested position of the particle is a little below the horizontal line. We believe this is due to the particle inertia, as when discarded, this phenomenon was not observed. While the particle is energetically nested at the position, the stress is applied by the ambient
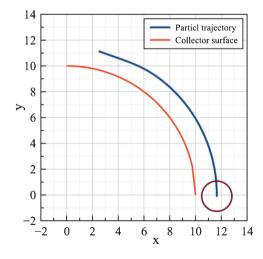

Figure 1. Trajectory of a particle attracted by a spherical collector, whose surface is shown in red. The blue line indicates the particle trajectory near the top of the collector. The direction of the unidirectional ambient flow is in the x-direction.
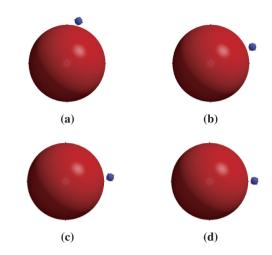
Figure 2. Snapshots of particle motion around the spherical collector: (a) intial position, (b) and (c) intermediate positions, and (d) nested position.

fluid flow on the particle surface, and this stress generates continuous angular motion at the nested position. Figure 2 shows four snapshots of the particle motion around the sphere. The six small black dots on the surfaces of the particle and collector indicate angular displacement as the particle moves while being influenced by van der Waals and hydrodynamic forces.[9] On the surface of the particle, relative fluid flow is assumed to be zero: no-slip boundary condition. Steady flow applies spatially uneven stress on the particle surface. As the energy is dissipated by the drag on the particle surface, the rotation (only) is generated as a response to the external fluid stress.

In this study, we simulated the hydrodynamic trapping of a small particle on the attractive collector surface. While van der Walls attraction and lubrication repulsion are balanced, the fine particle stays at a certain distance from the back hemisphere of the collector. Any fluid fluctuation or microscopic agitation may release the particle from the trapping. When a number of fine particles approach a collector, hydrodynamic shielding experienced by postcoming particles may enhance the hydrodynamic trapping. We are experimentally verifying this phenomenon, and preliminary data (unpublished) support our simulation results. To further investigate the realistic filtration phenomena at the microscopic level, the complex structure of granular packing, local fluid flow with strain, and polydispersity of fine particles must be considered, which will be our research topic in the near future.

References and Notes
1 K.-M. Yao, M. T. Habibian, C. R. O'Melia, *Environ. Sci. Technol.* **1971**, *5*, 1105.
2 V. Levich, *Physicochemical Hydrodynamics*, Prentice-Hall, Englewood Cliffs, N.J., **1962**, pp. 80–87.
3 J. T. Cookson, Jr., *Environ. Sci. Technol.* **1970**, *4*, 128.
4 R. Rajagopalan, C. Tien, *AIChE J.* **1976**, *22*, 523.
5 B. V. Derjaguin, L. Landau, *Acta Physicochim. URSS* **1941**, *14*, 633.
6 E. J. W. Verwey, J. Th. G. Overbeek, *Theory of the Stability of Lyophobic Colloids*, Elsevier, Amsterdam, **1948**.
7 N. Tufenkji, M. Elimelech, *Environ. Sci. Technol.* **2004**, *38*, 529.
8 K. E. Nelson, T. R. Ginn, *Langmuir* **2005**, *21*, 2173.
9 High-resolution images will be available by request to the corresponding author.